

## New theoretical approach of transition-metal impurities in semiconductors

C. Delerue, M. Lannoo, and G. Allan

*Laboratoire de Physique des Solides, Institut Supérieur d'Electronique du Nord, 41 boulevard Vauban, 59046 Lille Cédex, France*

(Received 7 July 1988)

A recently proposed self-consistent semiempirical tight-binding theory of substitutional transition-metal impurities in covalent and ionic semiconductors is described in detail. It is shown that it gives results with an accuracy comparable to that of local-density calculations and this has been achieved without the use of any adjustable parameters. Physical features are analyzed through a defect-molecule approach. Ionization energies are determined, allowing in several cases a direct comparison with experiments. The connection between level positions and band offsets at heterojunctions is discussed. Finally, the extension of this calculation to the photoionization cross sections is presented.

### I. INTRODUCTION

During the past ten years, important research has been engaged for a better understanding of the transition-metal (TM) impurities in semiconductors. These studies are justified by the particular and significant properties of these defects. TM ions create deep levels in most of the covalent and ionic semiconductors. With experiments like deep-level transient spectroscopy (DLTS) and electron paramagnetic resonance (EPR), several aspects of the behavior of  $3d$  impurities are now well known. First, although free TM atoms show ionization energies larger than 10 eV, several charge states can be localized in the band gap of the semiconductor, indicating a strong interaction between the defect and the medium. However, the multiplet spectra of  $3d$  impurities are quite similar to those of the free atoms and therefore have been described by the well-known Tanabe-Sugano diagrams.<sup>1</sup> We can add to this apparent conflictual behavior that the total spin of the EPR detected defects seems to obey Hund's rules, like the free atom, but electron-nuclear double resonance (ENDOR) data show an important spin delocalization.

The main features of these impurities are now beginning to be understood theoretically. Calculations of the electronic structure using cluster or Green's function approaches, and based on the local density or tight-binding approximations (see, for instance, Refs. 2–12) are able to give a clear idea of the electronic configuration of these defects but the corresponding levels are obtained with an accuracy not better than 0.3 eV.<sup>12</sup> Effects left down like multiplet splitting<sup>13</sup> lead to great difficulty in the interpretation of experimental data. Moreover, in spite of this progress, most properties of the TM impurities in III-V or in II-VI compound semiconductors remain unsatisfactorily explained as is pointed out in reviews like Ref. 14. Even recent local-density calculations lead to similar problems. Furthermore, they require heavy computations which are difficult to understand and which do not allow an easy extension to more complicated cases (see, for instance, Sec. V).

The aim of the present work is to discuss the trends in several physical properties on the basis of an extremely

simple and pedagogical molecular model, introduced in Ref. 8, and which will prove as successful as for the vacancy in silicon.<sup>15</sup> We also make use of the results of a self-consistent tight-binding Green's function calculation to predict trends in gap level positions and charge states for  $3d$  TM impurities in a variety of semiconductors. These results are comparable to those of the local-density (LD) calculations performed for Si and directly confirm the validity of the molecular description. The physical properties that will be discussed here are level positions and their relation with the charge state, ground-state spin configuration, relation between crystal field splitting and ionization energies, connection between TM impurity levels and heterojunction band offsets and, finally, the shape and magnitude of the optical cross sections as determined in deep-level optical spectroscopy (DLOS) experiments. The good agreement which will be obtained in all cases shows that our description is a correct starting point for investigating more complex effects like multiplet splitting.<sup>16</sup>

In the first part, we discuss the molecular model in its spin-restricted form and we recall briefly the basis of the renormalization concept. Secondly, we present the Green's function tight-binding calculation for the substitutional impurities. General results are discussed in the third part. Then we study the various charge states and we show the importance of a spin-unrestricted calculation. Finally, four applications of these calculations are proposed: (i) new empirical laws for the crystal-field splitting and ionization energies of TM ions in semiconductors are justified theoretically, (ii) optical cross sections are briefly described and compared with experiments, (iii) the connection between TM impurity levels and heterojunction band offsets is analyzed and, (iv) conclusions about TM impurities are used to derive simply the band structure of  $\text{CoSi}_2$ .

### II. RENORMALIZED MOLECULAR MODEL

We first recall the molecular model of TM substitutional impurities<sup>8</sup> based on a tight-binding approximation limited to a minimal atomic orbital basis set. The defect states result in the simplest view from the interaction of

the transition metal atom  $d$  states with the four dangling bonds of the Ga vacancy.<sup>17</sup> The  $d$  states, using symmetry considerations, are divided in two classes:  $e$ -like  $d$  orbitals remain uncoupled leading to very localized states in a more complete scheme (see Sec. III);  $t_2$ -like orbitals couple with the corresponding  $t_2$  state of the vacancy creating  $t_2$  bonding and  $t_2^*$  antibonding levels whose energies are given by the diagonalization of the following Hamiltonian:

$$\begin{pmatrix} E_d & V \\ V & E_v \end{pmatrix}, \quad (1)$$

where  $E_d, E_v$  are, respectively, the  $d$  and dangling bond state energies, and  $V$  is their coupling. We find easily the eigenvalues  $\epsilon_{t_2}$  and  $\epsilon_{t_2^*}$ :<sup>8</sup>

$$\epsilon_{t_2}^{t_2^*} = \bar{\epsilon} \pm (\delta^2 + V^2)^{1/2}, \quad (2)$$

with  $\bar{\epsilon} = (E_d + E_v)/2$  and  $\delta = (E_d - E_v)/2$ .

The eigenstates are

$$|t_2\rangle = \alpha|t_{2d}\rangle + \beta|t_{2v}\rangle, \quad (3)$$

$$|t_2^*\rangle = \beta|t_{2d}\rangle - \alpha|t_{2v}\rangle,$$

$$\alpha^2 = \frac{1}{2} \left[ 1 - \frac{\delta}{(\delta^2 + V^2)^{1/2}} \right], \quad (4)$$

with

$$\delta = \frac{\delta_0 + U_d/2(n_d - n_{d0} + 3) + (U_d - U_v)n_A/4 - U_v(3 - n_{v0})/2}{1 + \frac{(U_d + U_v)(6 - n_A)}{4(\delta^2 + V^2)^{1/2}}}, \quad (6)$$

which can be solved by iteration.

We will take a value of 8 eV for the Coulomb parameter  $U_d$ ,<sup>8</sup> but, as long as it is much larger than  $V$ , the exact value of this parameter is found to be unimportant for the accuracy of the results. The coupling parameter  $V$  is in a first step deduced from the empirical Harrison's rules.<sup>18</sup>

The molecular approach that we present here would be sufficient to explain the major physical features of the defect but would be inadequate to give quantitative values because of the effects left down. The main problem is the smallness of the cluster used. Picoli *et al.*<sup>8</sup> presented a renormalized defect molecule model which induces a modification of the previous parameters to take into account the rest of the crystal. This leads to a reduction of the coupling parameter  $V$  by the delocalization factor  $\gamma$ ,

$$V = \gamma V_0, \quad (7)$$

where  $V_0$  is the value calculated directly from Harrison's rules.<sup>18</sup> This reduction is due to the fact that the  $t_2$  level of the vacancy is not totally localized on the four dangling bonds. Thus the molecular model takes into account at least part of the effects of the medium on the impurity molecule. In these conditions, neglected effects are the interaction of the TM ion with the backbonds of the

$$\beta^2 = \frac{1}{2} \left[ 1 + \frac{\delta}{(\delta^2 + V^2)^{1/2}} \right].$$

Writing  $n_d = n_e + 6\alpha^2 + n_A\beta^2$  and  $n_v = 6\beta^2 + n_A\alpha^2$  for an electronic configuration  $t_2^6 e^{n_e} t_2^{*n_A}$ , the self-consistency can be simply achieved by imposing a linear dependence of the diagonal terms of the Hamiltonian with respect to the electronic population:

$$\begin{aligned} E_d &= E_{d0} + U_d(n_d - n_{d0}), \\ E_v &= E_{v0} + U_v(n_v - n_{v0}), \end{aligned} \quad (5)$$

where  $n_d, n_v$  are, respectively, the electronic populations on  $d$  orbitals and on dangling bond hybrids,  $U_d$  is the average Coulomb energy for  $d$  electrons,  $U_v$  is the effective Coulomb energy for the  $t_2$  state of the vacancy [ $U_v$  is usually very small compared to  $U_d$  (Ref. 8)].  $E_{d0}$  and  $E_{v0}$  are, respectively, the  $d$  orbital energy for the TM ion with  $n_{d0}$   $d$  electrons and the energy of the  $t_2$  state of the vacancy occupied by  $n_{v0}$  electrons (see Sec. III for details). This set of equations leads to the following one [if  $\delta_0 = (E_{d0} - E_{v0})/2$ ]:

four neighbors and with more distant neighbors. Nevertheless, as we show in the following, these effects are smaller so that, in any case, it does not seem necessary to include a third level to interpret the behavior of the main localized and resonant states as it has been suggested by Zunger.<sup>13</sup> The values of the parameters, the results obtained with the molecular model, are presented and justified in the Sec. IV.

### III. SEMIEMPIRICAL TIGHT-BINDING GREEN'S FUNCTION APPROACH

The aim of this part is first to present the Green's function calculation that we have performed here and secondly to give precisions about the set of parameters used in this semiempirical technique. The technique is based upon the Green's function theory in a tight-binding formalism. We start the computation with the calculation of the Green's functions for the perfect host crystal where the basis set consists of one  $s$  and three  $p$  states on each atom. The band structure of the crystal is obtained by the procedure described in Ref. 19 where interaction parameters up to second neighbors are taken into account. For II-VI compounds, we have derived our own set of parameters (see Table I). The Green's functions for

TABLE I. Parameters for the band structure of ZnSe and CdTe. As the spin orbit coupling is important in CdTe, we have taken an intermediate  $\Gamma$  point (notations of Ref. 19).

	$P$ (1)	$P$ (2)	$P$ (3)	$P$ (4)	$P$ (5)	$P$ (6)	$P$ (7)	$P$ (8)	$P$ (9)
CdTe	-8.5040	-0.9760	1.0520	4.1780	-5.0893	2.7170	4.4021	2.4481	4.7768
ZnSe	-9.5130	+0.0230	1.8200	5.5100	-5.7958	4.1185	5.0643	3.1667	6.2721
	$P$ (10)	$P$ (11)	$P$ (12)	$P$ (13)	$P$ (14)	$P$ (15)	$P$ (16)	$P$ (17)	$P$ (18)
CdTe	-0.5180	-0.6570	0.2776	0.2776	0.2590	0.3285	0.0000	0.0000	0.0000
ZnSe	-0.8165	-1.0885	0.6422	0.6422	0.4083	0.5443	0.0000	0.0000	0.0000
	$P$ (19)	$P$ (20)	$P$ (21)	$P$ (22)	$P$ (23)				
CdTe	0.0000	0.3401	0.3401	0.0000	0.0000				
ZnSe	0.0000	0.4499	0.4499	0.0000	0.0000				

the perfect crystal are calculated by integration over the Brillouin zone. When this is done we proceed in two steps: (i) we remove one atom (the cation in our case) to create the vacancy and (ii) we replace it by the metal ion. We use for this the Dyson equation:

$$G = G_0 + G_0 V G, \quad (8)$$

where  $G$  is the perturbed Green's function,  $G_0$  the host crystal Green's function, and  $V$  the perturbation matrix. The vacancy is obtained by applying an infinite potential on the removed atom.<sup>20</sup> The TM ion is represented as in the molecular case (see Sec. II) by its five  $d$  orbitals. The interatomic components of the interaction matrix  $V$  are deduced from Harrison's rules<sup>18</sup> for the first neighbors and are neglected for the others. The calculation is then performed self-consistently using the same linear dependence of the  $d$  energy  $E_d$  with the  $d$  electronic population  $n_d$  as for the molecular model:

$$E_d = E_{d0} + U_d(n_d - n_{d0}). \quad (9)$$

Finally, due to important screening effects in these semiconductors, we also impose for a defect in the neutral charge state the neutrality of the cell consisting of the TM ion and its four neighbors (see Ref. 21 for a discussion of the charge neutrality condition). We do not impose the neutrality of the TM ion directly because local screening within the cell is not as efficient as in the bulk crystal. The neutrality of the cell (i.e., the impurity and its four neighbors) is achieved by a potential on the four neighbors. In the same way, for a defect with a charge state  $q$ , we impose a net charge of  $q/\epsilon$  in this cell, where  $\epsilon$  is the dielectric constant. The self-consistency is then obtained after an iterative procedure, the  $d$  charge  $n_d$  being simply calculated by integration of the imaginary part of the Green's functions up to the Fermi level  $E_F$ . Finally, when self-consistency is achieved, the gap and resonant states are given by the following equation:

$$\text{Re}[\det(I - G_0 V)] = 0. \quad (10)$$

An important point in such a semiempirical technique is the justification of the parameters used. The validity of a given choice of parameters is measured by its success in the prediction of a broad range of physical properties.

Here we have chosen the empirical parameters and  $d^{-7/2}$  rules of Harrison<sup>18</sup> for the interatomic components of the matrix  $V$ . We will see in the following part that these empirical rules can directly deduced and justified by experimental data.<sup>22</sup> The main problem left is then to write the intra-atomic terms (the diagonal terms of the Hamiltonian matrix). We have assumed, as usually done in tight binding, that the atomic orbital energies are adequate for this calculation. We have thus taken  $E_{d0}$  and the average  $sp^3$  energy of the bulk crystal equal to the free atom values calculated with the Herman and Skillman technique.<sup>23</sup> For the TM atom,  $E_{d0}$  has been determined for the configuration  $d^{n-1}s^1$ . This can be qualitatively justified along the lines of Ref. 8 but we prefer to view it as a clear-cut semiempirical prescription to be tested by the overall success of the results. In this sense, our model is completely free of adjustable parameters.

A final comment should be made about our neglect of the impurity  $s$  and  $p$  states that might be important, for instance, in the case of Cu, where the  $d$  shell is filled. This is partially justified by our previous calculation for Si (Ref. 17) including these states and leading to almost exactly the same results as here for the gap states. This can be explained by the fact that the  $s$  state forms  $A_1$  bonding and antibonding states while  $p$  states only interact weakly with the  $T_2$  gap states for reasons given in Ref. 17. One can notice that the corresponding correction for the gap state is maximum for Cu and of order 0.2 eV.

#### IV. RESULTS OF THE SPIN RESTRICTED CALCULATIONS

The problem of TM impurities in Si has been extensively studied by various techniques, particularly by Zunger<sup>9,10,13</sup> using the local-density approach. Nevertheless, there is a need for simpler models to point out the main physical properties of TM impurities and to perform systematic analyses of trends. Furthermore, it is very interesting to see that tight-binding treatments can give trends with an accuracy comparable to what is obtained from the local-density approximation (we will see in the following that the comparison with experimental

data is similar) and in a much easier way.

In Fig. 1 are depicted the spin-restricted results from our Green's function calculations for the substitutional impurities in Si (solid line). The levels are populated in the low-spin-like configuration, i.e., we fill the  $e$  states before the  $t_2^*$  states (for details, see for instance, Ref. 24). Only the  $t_2$  bonding,  $t_2^*$  antibonding, and  $e$  levels are represented. The comparison with local-density results<sup>9</sup> is very good (the agreement is comparable to what is given in Ref. 17). The  $e$  level is, as predicted by the molecular model, very localized on the  $d$  orbitals of the transition atom (86% for Ti to 99% for Cu). The  $e$ -like  $d$  functions only couple to the backbonds of the nearest Si neighbors. The  $t_2$  bonding state is rather localized on the TM atom for the higher atomic weight, but for the lighter atoms, the system is found to be almost covalent (50% on the  $t_2$ -like  $d$  orbitals). The scheme for the  $t_2^*$  antibonding state is obviously inverted: for heavy atoms, this state is nearly the  $t_2$  level of the vacancy. For Cu, the  $d$  atomic level is very deep [ $-2.73$  eV from the valence band (VB) maximum] and we can consider the  $d$  atomic level and the  $t_2$  dangling bond state of the vacancy separately. The shape of the curve of Fig. 1 can be interpreted simply with the help of the defect molecule model. For Ti to Fe, the  $t_2^*$  level is empty, i.e.,  $n_A=0$  and only  $n_e$  varies. If we look at Eq. (6) the difference in energy  $2\delta$  between the  $e$  level and the  $t_2$  state of the va-

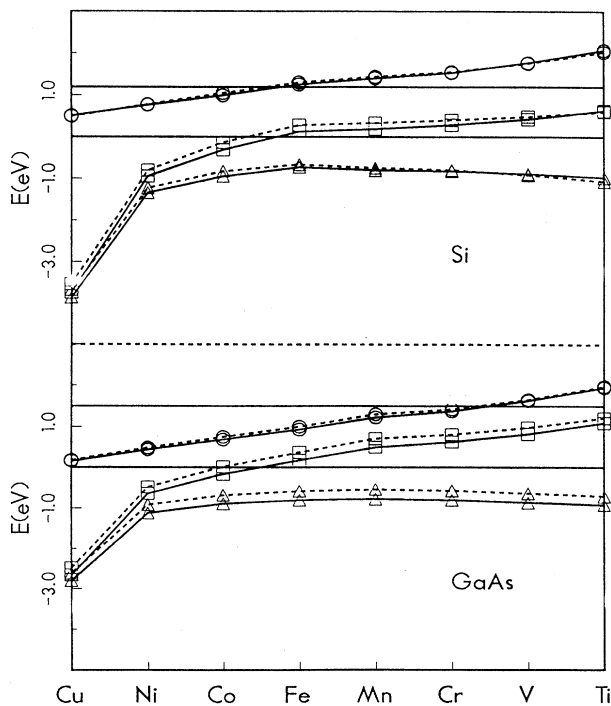


FIG. 1. Comparison of  $t_2$  ( $\Delta$ ),  $t_2^*$  ( $\circ$ ),  $e$  ( $\square$ ) levels for neutral TM ions of the 3d series in Si and GaAs obtained from the Green's function calculation (solid line) and the molecular model (dotted line).

cancy is fixed by two terms: the first one  $2\delta_0$  depends on the nature of the atom while the second part depends on  $n_d - n_{d0}$  which does not change. The quantity  $2\delta_0$  is a practically linear function of  $n_e$  with a slope of about 0.8 eV (see Table II). However, screening reduces this slope by a factor equal to the denominator in Eq. (6). For  $U_d \sim 8$  eV and  $V \sim 1$  eV this factor is about 12 leading to a slope of about 0.07 eV which corresponds to the results of Fig. 1.

Let us now discuss the validity of the defect-molecule model. In this model we have used exactly the same atomic energies as the full calculation (Table II). As the Green's function calculation predicts a small potential on the four neighbors in Si (typically 0.02 eV), we take for  $E_{v0}$  the  $t_2$  energy level of the vacancy without potential on the neighbors. The corresponding calculated values for  $E_{v0}$  are listed in the Table III. The comparison between molecular and Green's function results for Si in Fig. 1 is conclusive. The various levels are quasi similar in the two schemes. The  $e$ - $t_2^*$  splitting is very well described by the molecular model: this shows the efficiency of the renormalization<sup>8</sup> and of the concept of effective Hamiltonian.<sup>25</sup> This clearly demonstrates that the molecular model is able to give the major physical features of a defect.

Figure 1 also shows similar results for GaAs. In this case the molecular model gives  $e$  and  $t_2$  levels which are 0.2 eV higher than the corresponding levels from the Green's function calculation. This difference is due to the potential on the first neighbors which is equal to  $\approx -0.23$  eV in the case of GaAs. We have observed that the addition of this potential to the energy  $E_{v0}$  (reduced by the delocalization factor) gives results for the molecular model in very good agreement with Green's function values. This shows that long-range effects are not completely included in the renormalized molecular model. This point has been also verified for the other semiconductor compounds for which we have observed that the potential on the neighbors increases with the ionicity (and thus the disagreement between the molecular and the Green's function results). This is the main limitation of the molecular model. Nevertheless, this latter always contains the main physical characteristics of the defects.

TABLE II. Atomic energies of  $d$  orbitals for TM ions in a  $d^{n-1}s^1$  configuration and of  $s,p$  orbitals for semiconductor bulk atoms (all the values are in eV). All these values were calculated with the Herman and Skillman technique (Ref. 23).

	$E_{d0}$		$E_s$	$E_p$
		Si	-14.24	-7.03
Ti	-4.86	Ga	-11.39	-4.92
V	-5.70	As	-17.34	-7.92
Cr	-6.50	P	-17.03	-8.35
Mn	-7.28	In	-10.13	-4.69
Fe	-8.02	Sb	-14.82	-7.26
Co	-8.74	Cd	-7.70	-3.38
Ni	-9.44	Te	-17.11	-8.59
Cu	-10.12	Zn	-8.40	-3.38
		Se	-20.32	-9.53

TABLE III. Energy levels (in eV) for the cation vacancies in various semiconductors. Localization factors of the  $t_2$  levels on the first neighbors are also given.

	$a_1$ (eV)	$t_2$ (eV)	Localization
Si	-0.68	0.36	60%
GaAs	-0.39	0.06	47%
GaP	-0.28	0.38	63%
InP	0.37	0.67	57%
ZnSe	0.17	0.78	66%
CdTe	-0.18	0.16	60%

In any case, the molecular model is a very good tool whenever one needs to point out particular trends in the properties of TM ions in semiconductors (see, for example, a recent application, Ref. 26).

The one-electron levels of TM impurities in III-V and II-VI compound semiconductors almost show the same behavior as in Si and their characteristics are similar. Nevertheless, as gaps in ionic semiconductors are often wider than the Si gap, more than one localized state can be seen. Moreover, we have observed an increase of the localization of the  $t_2^*$  levels on the  $d$  functions in II-VI compounds ( $\approx 80\%$  for Cr in ZnSe). Recently, Martinez<sup>27</sup> reached the same conclusion from an analysis of optical cross sections. Comparison with results from various authors is also impressive. Singh and Zunger<sup>28</sup> have calculated acceptor levels for the  $3d$  series from Cr to Zn in GaP with their self-consistent quasiband crystal-field Green's function method. For example, they found localization factors on the  $d$  orbitals for the  $t_2^*$  level of 2% for GaP:Cu and 50% for GaP:Fe while we find, respectively, 4% for Cu and 58% for Fe in our work.

### V. SPIN POLARIZED APPROACH—COMPARISON WITH EXPERIMENT

Transition-metal atoms are subject to important many-electron phenomena which do not disappear when they are introduced in the crystal. This leads to multiplet spectra which will be studied in another paper.<sup>16</sup> In the one-electron approximation used here, it is important to carry on an unrestricted treatment of the problem in order to examine the importance of the exchange terms on the self-consistency of the system. We will see that the simplicity of our algorithms allows us to perform for the first time, to our knowledge, calculations for all the transition series in III-V and II-VI semiconductors (Vogl and Baranowski<sup>7</sup> first used a tight-binding approach through an Anderson Hamiltonian theory which includes a rather large number of parameters and diverges somehow from the results of more recent calculations).

Our spin polarized treatment has been previously developed by Picoli *et al.*<sup>8</sup> in the defect-molecule model. In this treatment the spin-dependent atomic energies of the  $d$  states are written under the form

$$E_{d\uparrow} = E_{d0} + U_d(n_d - n_{d0}) - \frac{J}{2}(n_{d\uparrow} - n_{d\downarrow}),$$

$$E_{d\downarrow} = E_{d0} + U_d(n_d - n_{d0}) + \frac{J}{2}(n_{d\uparrow} - n_{d\downarrow}),$$
(11)

TABLE IV. Calculated values for the average exchange interaction  $J$  [see Eq. (12)]. Racah parameters  $B$  and  $C$  (Ref. 29) are derived from Ref. 30 (all the values are in meV).

	Ti	V	Cr	Mn	Fe	Co	Ni
$B$	85	83	89	109	108	110	130
$C$	310	302	349	391	455	479	539
$J$	376	367	411	478	522	543	622

where  $J$  is the average exchange integral between two different orbitals. Using the Racah parameters<sup>29</sup>  $A$ ,  $B$  and Griffith's tables,<sup>30</sup> we obtain<sup>31</sup>

$$J = \gamma(\frac{5}{2}B + C),$$
(12)

where  $\gamma$  is a reduction term taking in account solid-state effects<sup>8</sup> (we keep the value  $\gamma = 0.72$  of Ref. 8). The values for  $J$  are summarized in Table IV.

The previous equations can be solved self-consistently both for the defect molecule and the Green's function calculations. In the case of the molecular model, this leads to a simple combined resolution of two  $2 \times 2$  Hamiltonians. Due to the simplicity of the algorithms (even for the Green's function model), we have obtained all the spin-unrestricted results from Si to CdTe. We have also undertaken calculations for the maximum and the minimum spin configurations when possible. The  $e$  and  $t_2^*$  antibonding levels from the Green's function calculation are plotted in Fig. 2 for Si and 3 for CdTe. Simple interpretations of these curves can be given directly by using the molecular model. Figure 2 (spin-unrestricted results for Si) can be separated into two parts, Fe being at the boundary. For the lighter atoms, the exchange split-

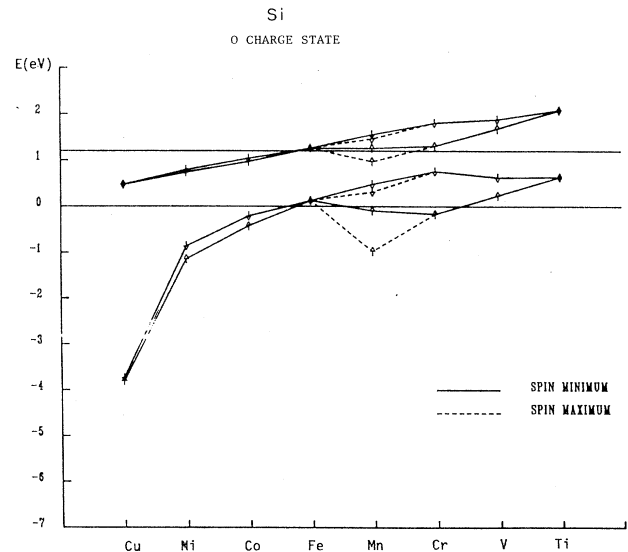


FIG. 2. Results from spin-polarized Green's function calculations for neutral TM ions in Si. Only the  $e$  and  $t_2^*$  levels are represented ( $\uparrow$  spin up,  $\downarrow$  spin down). The high spin configuration (dotted lines) is only obtained for Mn.

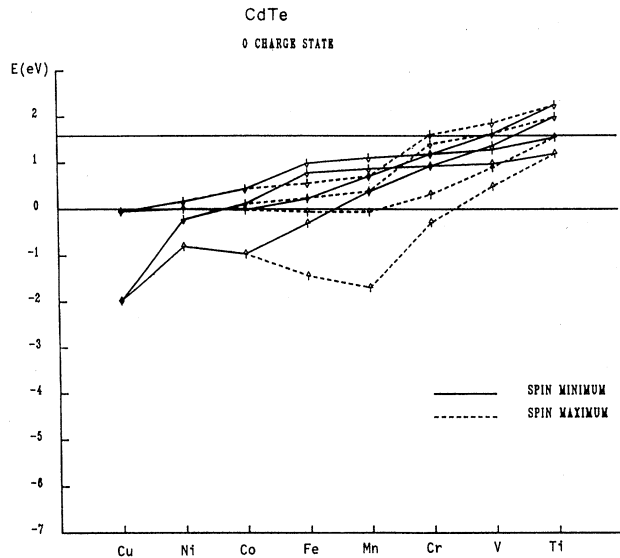


FIG. 3. Results from spin-polarized Green's function calculations for neutral TM ions in CdTe (same notations as Fig. 2). In all the cases, the high spin configuration is obtained.

ting is rather strong for the  $e$  levels but is sensibly reduced for the  $t_2^*$  levels. The  $e$  level is very localized on  $d$  orbitals, and therefore, an asymmetric population of the  $e_{\uparrow}$  and  $e_{\downarrow}$  levels will lead to a large splitting. The  $t_2^*$  splitting is reduced due to the important hybridization with the  $sp^3$  orbitals which are less spin polarizable (we

neglect this effect in our approach). This is also the reason for the small exchange splitting for the heavy TM atoms for which the  $e$  levels are completely filled. We were only able to obtain a maximum spin configuration for Mn in Si (Mn is the only experimentally observable substitutional TM impurity in silicon to our knowledge).

Beeler *et al.*<sup>11</sup> calculated the substitutional TM impurity levels in an unrestricted muffin-tin orbital technique which gives essentially the same results but with a larger exchange splitting for the  $t_2^*$  level. For CdTe (Fig. 3) and the other ionic compounds, a high spin configuration is often found due to the decrease of the crystal-field splitting. The sole exception to the Hund's rule is found for neutral Co in GaAs, GaP, and InP for which a low spin configuration is imposed by the presence of the  $e$  levels in the valence band. It is interesting to note that neutral cobalt has not yet been observed experimentally. The exchange splitting parameter is increasing in III-V and II-VI compound semiconductors. This fact is related to the increase of the  $t_2$  localization on the  $d$  orbitals (particularly for II-VI compounds).

To our knowledge, there is only one other work concerning TM impurities in III-V compounds in an unrestricted form, from Katayama-Yoshida *et al.*<sup>32</sup> treating GaAs:V for  $V^{3+}$  and  $V^{2+}$ . They obtain a mean position of the  $e$  level close to ours but their exchange splitting is larger by a factor of 2. In spite of this, they conclude that  $V^{2+}$  is low-spin-like because of the localization of the two  $t_2^*$  levels in the conduction band. We do not get the same conclusion because our  $t_{2\uparrow}^*$  level lies within the gap. They find an exchange splitting for the  $t_2^*$  state that is practically negligible. This means that their antibonding level has no  $d$  character on the impurity and is totally

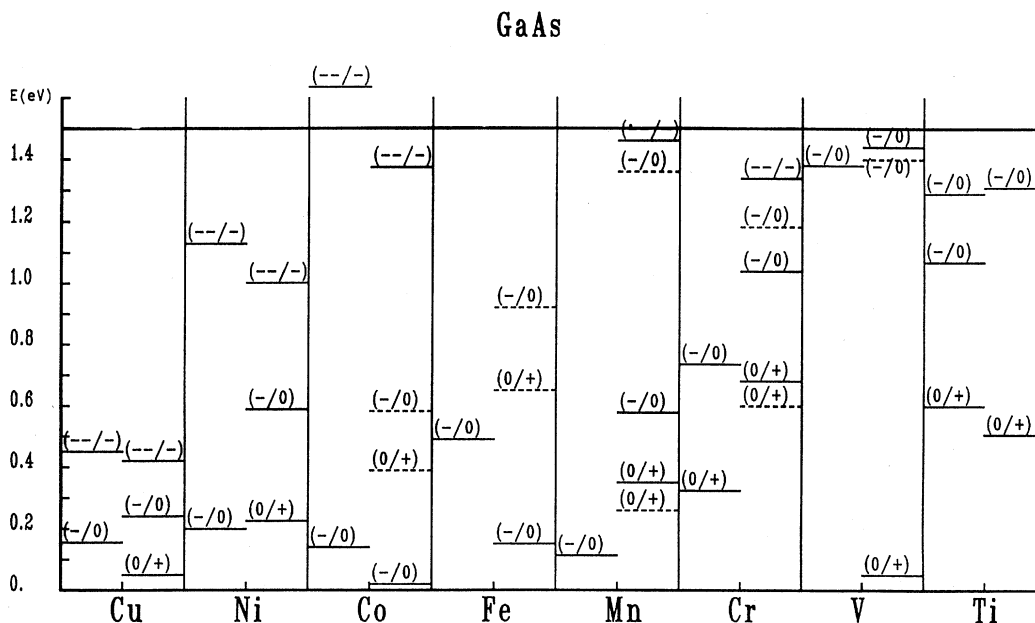


FIG. 4. TM impurity levels in GaAs. The right-hand side shows the theoretical levels (dashed line for low spin configuration, solid line for high spin). The left part is devoted to the experimental results (dashed line for internal transitions).

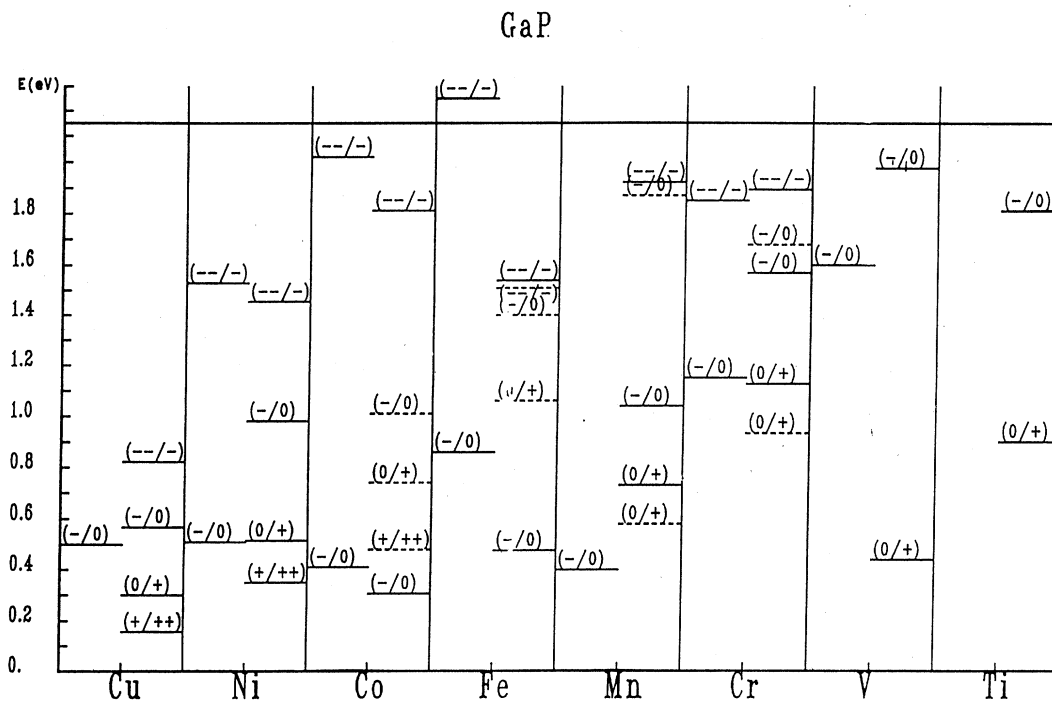


FIG. 5. Same as Fig. 4 for GaP.

localized on the dangling bonds. It is also surprising that the  $t_2^*$  level position is invariant for the two charge states. All these facts are in disagreement with our calculation and with their conclusions for GaP.

One purpose of the present work is to predict theoretical ionization energies and compare them with experi-

mental data. Using the Slater transition state, we calculate these energies for both low and high spin configurations. The results are given in Figs. 4–8 for GaAs, GaP, InP, ZnSe, and CdTe. For each Tm, the right-hand side shows the theoretical levels (dashed lines for low spin configurations), and the left-hand side the ex-

### InP

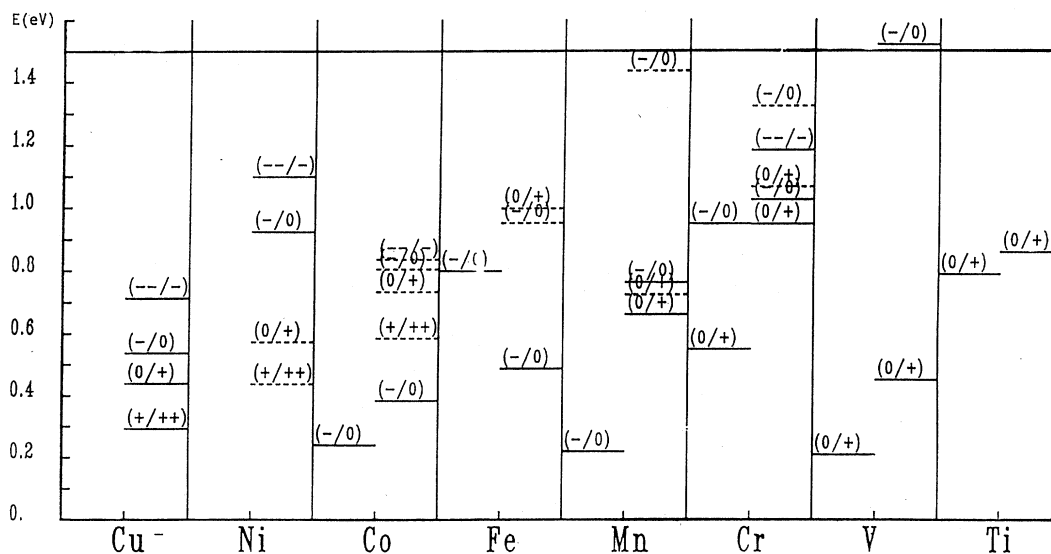


FIG. 6. Same as Fig. 4 for InP.

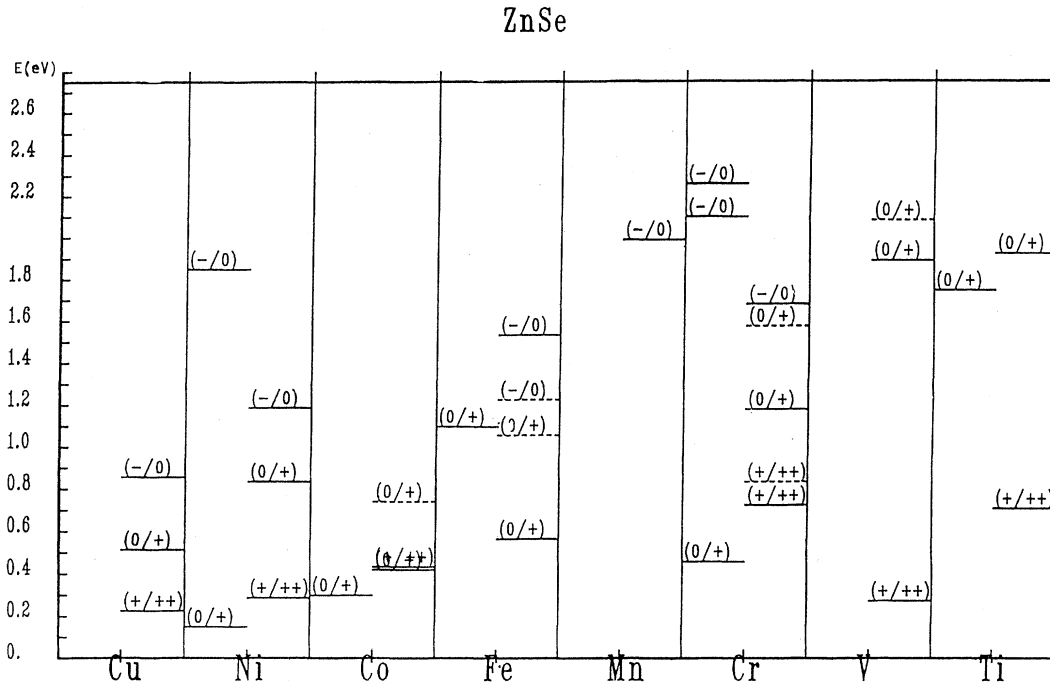


FIG. 7. Same as Fig. 4 for ZnSe.

perimental values (dashed lines for internal transitions). These experimental values are mainly deduced from the compilations by Clerjaud<sup>14</sup> and Zunger.<sup>13</sup> First, it is convenient to discuss the levels which are directly comparable with experimental data, i.e., for which our spin-unrestricted treatment is expected to work (i.e., where the

$e$  and  $t_2^*$  orbitals are populated by only one or two electrons). It is the case for donor levels of Ti, double acceptor levels of Cu in III-V semiconductors, and acceptor levels of Cu in II-VI compounds.

Concerning the donor levels of Ti, experimental data are available only in GaAs and InP: we find a very good

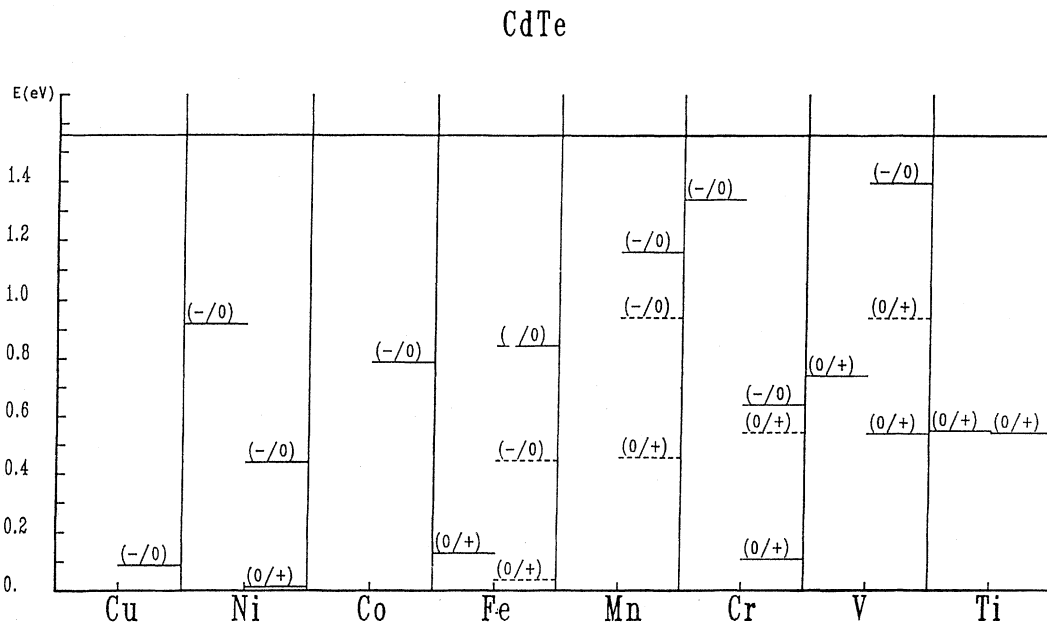


FIG. 8. Same as Fig. 4 for CdTe.



TABLE V. Predicted energy levels obtained from a compilation of calculated and experimental levels (see text). An interrogation mark following the value (in eV) means that the prediction is more doubtful.

GaP	InP	ZnSe
Cu(---/-) 0.82	Cu(---/-) 0.71	V(0/+) 2.10
Cu(0/+) 0.30?	Cu(-/0) 0.50	Ti(+ / + +) 0.71
Ti(0/+) 0.90	Cu(0/+) 0.35?	Cu(-/0) 0.85
Ti(-/0) 1.81	V(-/0) 1.40?	Cu(0/+) 0.51
V(0/+) 0.25	Cr(0/+) 0.62	Cu(+ / + +) 0.22
Cr(0/+) 0.80	Cr(---/-) 1.30?	
	Ni(-/0) 0.45?	
	Ni(---/-) 1.20	

agreement with a mean error inferior to 0.1 eV. Furthermore, the double acceptor level of Cu in GaAs is predicted very accurately (0.03 eV between theory and experiment). We have found previously that the  $t_2^*$  level of Cu is very localized on the dangling bond states so that the multiplet corrections will be weak. This explains why in GaAs and GaP the agreement for the Cu acceptor level is better than 0.1 eV. All these results are very satisfying and prove the efficiency of a tight-binding approach, even for numerical and quantitative calculations. We can also note that Singh *et al.*<sup>28</sup> have obtained acceptor levels in GaP very close to ours.

It is then possible to predict several levels. First, for Cu, levels can be found in GaP and InP in the lower part of the gap. In GaP, a donor level is predicted for Ti at 0.9 eV: the good agreement for these levels in GaAs can give confidence in these predictions. A double donor level for Ti in ZnSe at 0.70 eV seems also realistic. Another important point to emphasize is that the positions of experimental levels with respect to the theoretical ones are similar in all isovalent compounds. In effect, it is reasonable to consider that multielectron effects will be equivalent for a given level in various semiconductors, provided that the electronic properties of these compounds are close together. Therefore, using the fact that in GaAs and GaP, predicted double acceptor levels for Ni are localized at  $\sim 0.1$  eV under the experimental values, we can easily predict the same level in InP at 1.2 eV (calculated level: 1.1 eV). Table V summarizes some predicted levels obtained by this procedure. Other levels can be expected to lie in the band gap but their energy cannot be given for the moment with a sufficient accuracy (for example, an acceptor level for Mn in ZnSe and CdTe is probable; see Figs. 4–8).

## VI. SOME APPLICATIONS OF THE GREEN'S FUNCTION CALCULATION

We have seen that the complete semiempirical tight-binding Green's function calculation gives results whose accuracy is comparable with local-density ones. The relative simplicity of the algorithms and the direct correspondence with the defect-molecule model allow us to consider a wide range of applications. We propose here four such applications which are developed in other publications.

### A. New universal empirical laws

Recently, two new empirical laws for the crystal-field splitting  $\Delta$  and the ionization energy  $E_I$  of transition-metal ions in semiconductors have been justified theoretically.<sup>22</sup> The first one concerns the product  $E_I\Delta$  which turns out to be proportional to  $d^{-7}$  where  $d$  is the interatomic distance, at least for a given impurity in different semiconductors. This rule has been verified experimentally for various semiconductors.<sup>22</sup> Figure 9 shows that this rule is effectively justified by the Green's function results. This law can be understood directly on the basis of the molecular model. We have seen in the first part that,

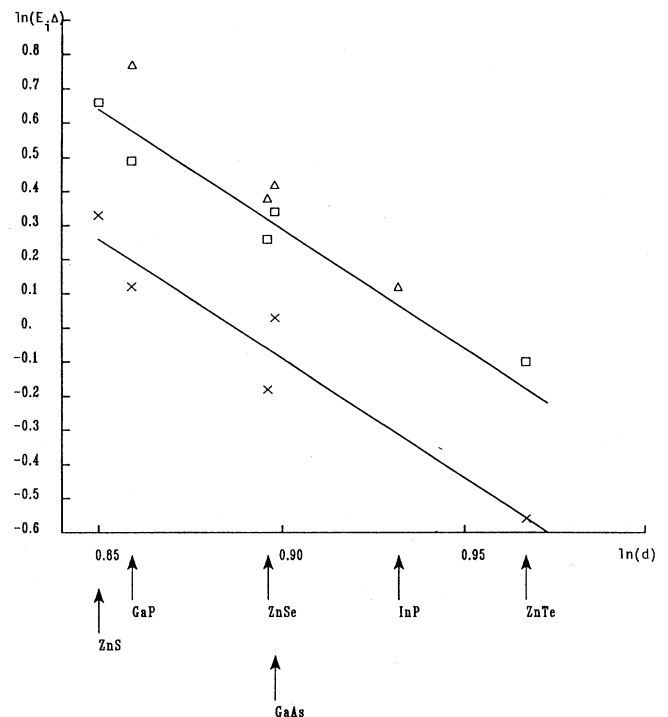


FIG. 9. Plot of  $\ln[E_I \Delta (\text{eV}^2)]$  versus  $\ln[d (\text{\AA})]$  ( $d$  interatomic distance) where  $\Delta$  is the energy of the zero-phonon line of the transition  ${}^5T_2 \rightarrow {}^5E$  for  $\text{Cr}^{2+}$  ( $\square$ , experimental;  $\Delta$ , calculated) and  ${}^4A_2 \rightarrow {}^4T_2$  for  $\text{Co}^{2+}$  ( $\times$ ) in various semiconductors.

first part that, in the molecular model, each  $t_2$ -like  $d$  orbital can be treated separately. Then the wave function  $\psi$  can be written as

$$\psi = a_d \Phi_d + \sum_{\alpha} a_{\alpha} \Phi_{\alpha}, \quad (13)$$

where  $\Phi_d$  is one of the  $d$  orbitals and the  $\Phi_{\alpha}$  belong to the remaining crystal. It is easy to show that the eigenstates of the Hamiltonian follow the equation

$$E = E_d + \sum_{\alpha} \frac{|V_{d\alpha}|^2}{E - E_{\alpha}}, \quad (14)$$

where  $E_{\alpha}$  is the energy of the state  $\Phi_{\alpha}$  and  $V_{d\alpha}$  is the coupling term between  $\Phi_d$  and  $\Phi_{\alpha}$ . As the neighbors of the TM ion are the anions and the  $t_2$ -like combinations of the anion states mainly belong to the top of the valence band  $E_v$ , we can approximately replace  $E_{\alpha}$  by  $E_v$  (this corresponds to another manner of building a molecular model), which leads to

$$(E - E_d)(E - E_v) = \sum_{\alpha} |V_{d\alpha}|^2. \quad (15)$$

As the crystal-field splitting is equal to  $\Delta = E - E_d$  and the ionization energy from the valence band to  $E_I = E - E_v$ , we obtain finally

$$E_I \Delta = \sum_{\alpha} |V_{d\alpha}|^2. \quad (16)$$

Applying Harrison's empirical rules,<sup>18</sup> in which  $V_{d\alpha}$  varies as  $d^{-7/2}$ ,  $E_I \Delta$  will vary as  $d^{-7}$ . Therefore, Harrison's laws receive a direct experimental confirmation.

The second empirical law described in Ref. 22 shows that the crystal-field splitting varies linearly with the bulk Phillip's ionicity.<sup>33</sup> Figure 10 clearly makes evident the validity of this law for  $\text{Cr}^{2+} ({}^5T_2 \rightarrow {}^5E)$  and  $\text{Co}^{2+} ({}^4A_2 \rightarrow {}^4T_2)$  internal transitions. In the same figure, corresponding calculated crystal-field splittings show the same linear dependence (with a constant shift which is due to the multielectrons effects). A simple analytical formula can be obtained for this law again on the basis of the molecular model of Sec. I in the approximation of a strong screening, i.e., we suppose that the TM ion is neutral. In this extreme case, the crystal-field splitting is fixed entirely by the bulk ionicity with a quasilinear dependence. This empirical law still confirms the importance of screening effects. We again see that the molecular model gives good tendencies and provides the right physical interpretation.

### B. Optical cross sections

A new approach to the calculation of the optical cross sections has been recently applied to the case of the vacancy in silicon.<sup>34</sup> This is based on a tight-binding Green's function formalism for the electronic part (i.e., without electron-lattice interaction) of the optical cross section. We have applied this formalism to the case of the TM substitutional impurities in semiconductors. A complete study of the optical cross sections of the  $3d$

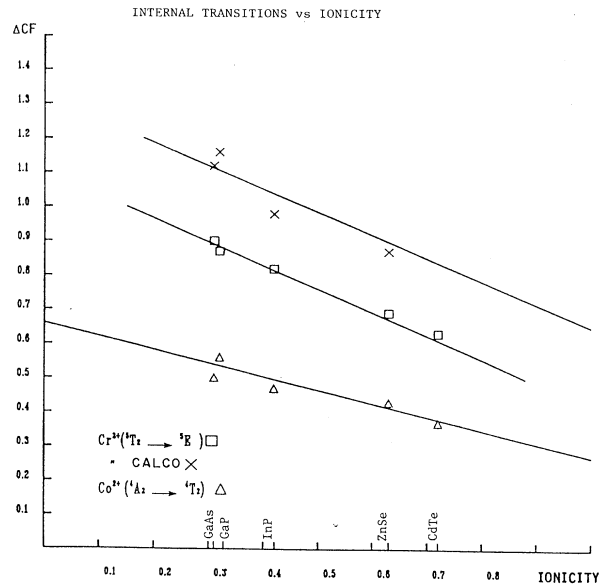


FIG. 10. Relationship between the effective crystal-field splitting and the ionicity for  $\text{Cr}^{2+} ({}^5T_2 \rightarrow {}^5E)$  ( $\square$ , experimental;  $\times$ , calculated) and for  $\text{Co}^{2+} ({}^4A_2 \rightarrow {}^4T_2)$  ( $\triangle$ , observed).

series in InP has been performed. Detailed results are published elsewhere.<sup>35,36</sup> This new approach allows us to calculate directly the absolute value of the optical cross section versus frequency which can be compared with the experimental one. We will see that the comparison between theory and experiment can definitely give support to a model for the electronic configuration of a defect.

The shape of the experimental optical cross sections contains information about the transitions from the defect levels (fundamental or excited) to the bands or about the presence of internal transitions. The analysis of the absolute values can be related to the nature of the wave function of the defect.<sup>27</sup> The direct comparison in Fig. 11 between theoretical and experimental spectra is also a test for the validity of a given model. Let us, for instance, in Fig. 11 discuss the optical cross section spectra for  $\text{Ti}(0/+)$  in InP. The  $\sigma_n$  spectra (transition of an electron from the defect to the conduction band) shows an important peak centered around 0.62 eV. We do not observe it on our theoretical spectra of a transition with the conduction band. This peak is in fact correlated with an internal transition (here  ${}^2E \rightarrow {}^2T_2$ ) in the final state: the addition of this internal transition leads to a very good agreement between theory and experiment. The optical threshold at  $\sim 1.3$  eV is associated with the transition to the bottom of a conduction band ( $L_1$ ). The weak absolute value for  $\sigma_n$  ( $10^{-17}$  cm<sup>2</sup>) is evidence of the involvement of the  $e$  level as predicted by the calculations.<sup>27,35,36</sup> Such an analysis can be pursued for the entire  $3d$  series:<sup>35,36</sup> we have been able to show, for instance, that the observed optical cross section for  $\text{Co}(-/0)$  is not

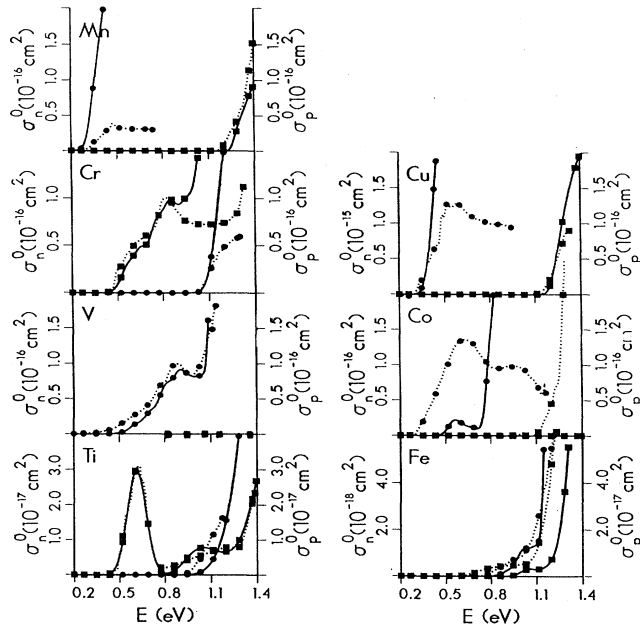


FIG. 11. Absolute photoionization cross-section spectra  $\sigma_n^0$  and  $\sigma_p^0$  [the theoretical spectra are in solid lines, experimental in dotted lines, (●)  $\sigma_p^0$  and (■)  $\sigma_n^0$ ].

consistent with an electron on an  $e$  orbital involved in the transition.

### C. TM impurities and band offsets at semiconductor heterojunctions

A novel empirical approach for the prediction of band offsets at semiconductor heterojunctions has been recently proposed.<sup>37</sup> In this approach the valence band discontinuity would be given by just the difference in energy level positions of a TM impurity in the two compounds forming the heterojunction. This was based upon the observation that TM impurity levels can be aligned in isovalent semiconductors, i.e., that it is possible to align all the levels of TM impurities by a simple shift of the corresponding band structures. Up to now, there was no theoretical proof of this new empirical rule. Figure 12 shows the plot of several TM levels in III-V compound semiconductors. Valence band edges are shifted with respect to one another so that the mean square deviation between corresponding levels is minimized. The obtained band offsets are found to be 0.11, 0.39, and 0.96 eV for InP/GaP, GaAs/GaP, and CdTe/ZnSe, respectively, in excellent agreement with the values deduced from experiment<sup>37</sup> (0.17, 0.33, and 0.80 eV, respectively).

Two physical explanations for this correlation were given recently. First, Zunger and co-workers<sup>38</sup> argued that the TM impurity levels could be pinned to the vacu-

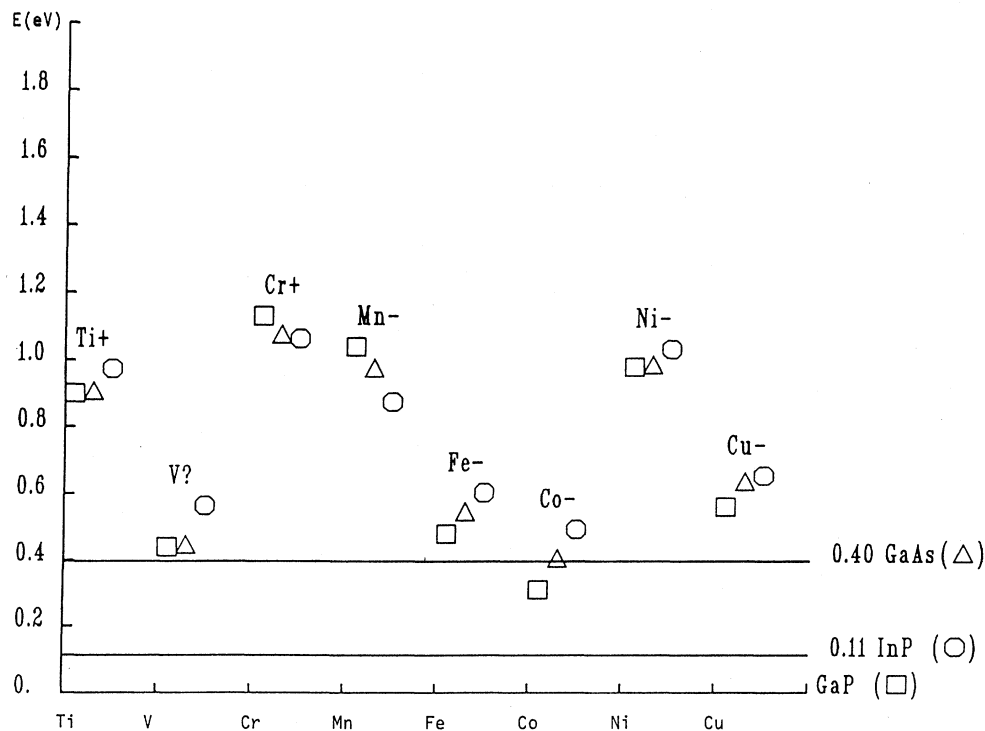


FIG. 12. Some calculated energy level for  $3d$  ions in III-V materials. The valence band edges are shifted in such manner that the average mean square deviation between the corresponding levels in isovalent semiconductors is minimized (GaP taken as reference).

um level. We have shown recently that this is neither experimentally, nor theoretically justified.<sup>39</sup> Secondly, Tersoff and Harrison<sup>26</sup> have used the molecular model developed previously to show that the Tm levels are pinned to the  $t_2$  state of the vacancy. At the same time, they try to demonstrate that the band discontinuity at heterojunctions also corresponds to an alignment of the  $t_2$  levels of the cation vacancies. Their latter argument was not very conclusive and we have shown that the TM levels are pinned to the average dangling bond level (this is due to the potential on the four nearest neighbors which increases the influence of the whole crystal and, as we have seen in the first part, this effect cannot be accounted for the molecular model). In a recent paper, Lefebvre *et al.*<sup>40</sup> have clearly established that a semiconductor heterojunction is characterized by the alignment of the respective average dangling bond levels of each semiconductor. Therefore, the TM alignment at heterojunctions is plainly justified.

#### D. Band structure of TM compounds

The use of atomic energies and semiempirical rules for the interaction parameters in the determination of the electronic properties of TM impurities in semiconductors gives remarkable results. This success is of great interest for numerous expectable applications. It is, for example, interesting to verify if such a semiempirical procedure could be applied to the determination of the band structure of TM metal compounds. We have calculated the band structure of CoSi<sub>2</sub> using the tight-binding method of Slater and Koster.<sup>41</sup> The interatomic parameters are considered only up to second nearest-neighbors interactions. We have used for this the semiempirical rules of Harrison.<sup>18</sup> The energies of Co and Si are the atomic ones listed in Table II. The structure which is obtained in this way is given in Fig. 13 for the main directions in reciprocal space. It compares favorably with the band structure calculated in Ref. 42.

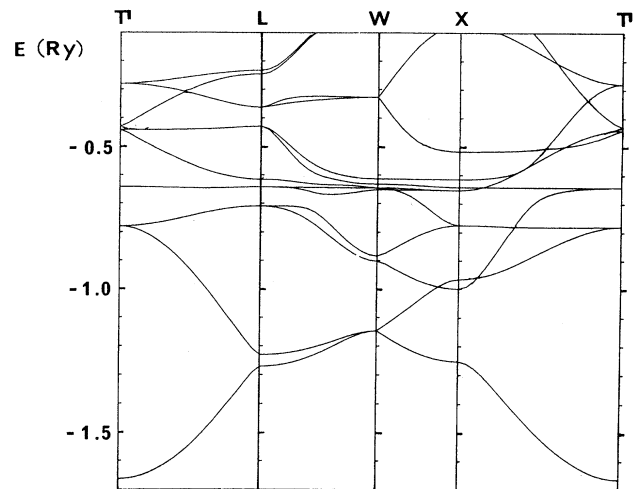


FIG. 13. Band structure of CoSi<sub>2</sub>. Parameters used are given in the text.

## VII. CONCLUSION

A general study of substitutional TM impurities in the most common semiconductors has been carried out within a charge-dependent tight-binding framework. The simplicity of the algorithms transforms the models used into efficient theoretical tools for further studies as has been demonstrated through recent applications. We have shown that a semiempirical tight-binding method can give quantitative results, and, at the same time that a molecular model provides in a rather simple way clear explanations on the physics of TM impurities in semiconductors.

<sup>1</sup>S. Sugano, Y. Tanabe, and H. Kaminura, *Multiplets of Transition-Metal Ions in Crystals* (Academic, New York, 1970).

<sup>2</sup>L. A. Hemstreet, *Phys. Rev. B* **15**, 834 (1977).

<sup>3</sup>L. A. Hemstreet and J. O. Dimmock, *Phys. Rev. B* **20**, 1527 (1979).

<sup>4</sup>G. G. Deleo, G. D. Watkins, and W. B. Fowler, *Phys. Rev. B* **23**, 1851 (1981).

<sup>5</sup>A. Fazio and J. R. Leite, *Phys. Rev. B* **21**, 4710 (1980).

<sup>6</sup>P. Pêcheur and G. Toussaint, *Proceedings of the 12th International Conference on Defects in Semiconductors*, edited by C. A. J. Ammerlan (North-Holland, Amsterdam, 1983), p. 112.

<sup>7</sup>P. Vogl and J. Baranowski, 17th International Conference on the Physics of Semiconductors, 1985 (unpublished).

<sup>8</sup>G. Picoli, A. Chomette, and M. Lannoo, *Phys. Rev. B* **30**, 7138 (1984).

<sup>9</sup>A. Zunger and U. Lindefelt, *Phys. Rev. B* **27**, 1191 (1983).

<sup>10</sup>H. Katayama-Yoshida and A. Zunger, *Phys. Rev. B* **31**, 7877 (1985).

<sup>11</sup>F. Beeler, O. K. Andersen, and M. Scheffler, *Phys. Rev. Lett.* **55**, 1498 (1985).

<sup>12</sup>M. Lannoo, *J. Phys. C* **17**, 3137 (1984).

<sup>13</sup>A. Zunger, *Solid State Phys.* **39**, 275 (1986).

<sup>14</sup>B. Clerjaud, *J. Phys. C* **18**, 3615 (1985).

<sup>15</sup>M. Lannoo and J. Bourgoin, *Point Defects in Semiconductors I*, edited by M. Cardona (Springer, Berlin, 1981).

<sup>16</sup>C. Delerue and M. Lannoo (unpublished).

<sup>17</sup>C. Delerue, G. Allan, and M. Lannoo, *Proceedings of the 14th International Conference on Defects in Semiconductors*, edited by H. J. von Bardeleben (Trans Tech, Aedermansdorf, Switzerland, 1986), Vols. 10–12, p. 34.

<sup>18</sup>W. A. Harrison, *Electronic Structure and the Properties of Solids: The Physics of the Chemical Bond* (Freeman, New York, 1980).

<sup>19</sup>D. N. Talwar and C. S. Ting, *Phys. Rev. B* **25**, 2660 (1982).

<sup>20</sup>M. Lannoo and P. Lengart, *J. Phys. Chem. Solids* **30**, 2409 (1969).

<sup>21</sup>C. Priester, G. Allan, and M. Lannoo, *Phys. Rev. B* **33**, 7386

- (1986).
- <sup>22</sup>Z. Liro, C. Delerue, and M. Lannoo, *Phys. Rev. B* **36**, 9362 (1987).
- <sup>23</sup>F. Herman and S. Skillman, *Atomic Structure Calculations* (Prentice Hall, New York, 1963).
- <sup>24</sup>G. W. Ludwig and H. H. Woodbury, *Solid State Phys.* **13**, 223 (1962).
- <sup>25</sup>M. Lannoo, *Handbook of Surfaces*, edited by L. Dobrzynski (Garland, STPM, New York, 1978), Vol. 1, p. 11.
- <sup>26</sup>J. Tersoff and W. A. Harrison, *Phys. Rev. Lett.* **58**, 2367 (1987).
- <sup>27</sup>G. Martinez, *Proceedings of the 14th International Conference on Defects in Semiconductors*; edited by H. J. von Bardeleben (Trans Tech, Aedermansdorf, Switzerland, 1986), Vols. 10–12, p. 603.
- <sup>28</sup>V. Singh and A. Zunger, *Phys. Rev. B* **31**, 3729 (1985).
- <sup>29</sup>G. Racah, *Phys. Rev.* **63**, 367 (1943).
- <sup>30</sup>J. S. Griffith, *The Theory of Transition-Metal Ions* (Cambridge University Press, Cambridge, 1971).
- <sup>31</sup>B. H. Brandow, *Adv. Phys.* **26**, 651 (1977).
- <sup>32</sup>H. Katayama-Yoshida and A. Zunger, *Phys. Rev. B* **33**, 2961 (1983).
- <sup>33</sup>J. C. Phillips, *Rev. Mod. Phys.* **42**, 317 (1970).
- <sup>34</sup>J. Petit, G. Allan, and M. Lannoo, *Phys. Rev. B* **33**, 8595 (1986).
- <sup>35</sup>G. Bremond, G. Guillot, A. Nouailhat, C. Delerue, and M. Lannoo (unpublished).
- <sup>36</sup>C. Delerue, M. Lannoo, G. Bremond, G. Guillot, and A. Nouailhat (unpublished).
- <sup>37</sup>J. M. Langer and H. Heinrich, *Phys. Rev. Lett.* **55**, 1414 (1985).
- <sup>38</sup>M. J. Caldas, A. Fazzio, and A. Zunger, *Appl. Phys. Lett.* **45**, 671 (1984).
- <sup>39</sup>C. Delerue, M. Lannoo, and J. M. Langer, *Phys. Rev. Lett.* **61**, 199 (1988).
- <sup>40</sup>I. Lefebvre, M. Lannoo, C. Priester, G. Allan, and C. Delerue, *Phys. Rev. B* **36**, 1336 (1987).
- <sup>41</sup>J. C. Slater and G. F. Koster, *Phys. Rev.* **94**, 1498 (1954).
- <sup>42</sup>W. R. Lambrecht, N. E. Christensen, and P. Bloch, *Phys. Rev. B* **36**, 2493 (1987).